Report

Current Biology

General Visual and Contingent Thermal Cues Interact to Elicit Attraction in Female *Aedes aegypti* Mosquitoes

Graphical Abstract

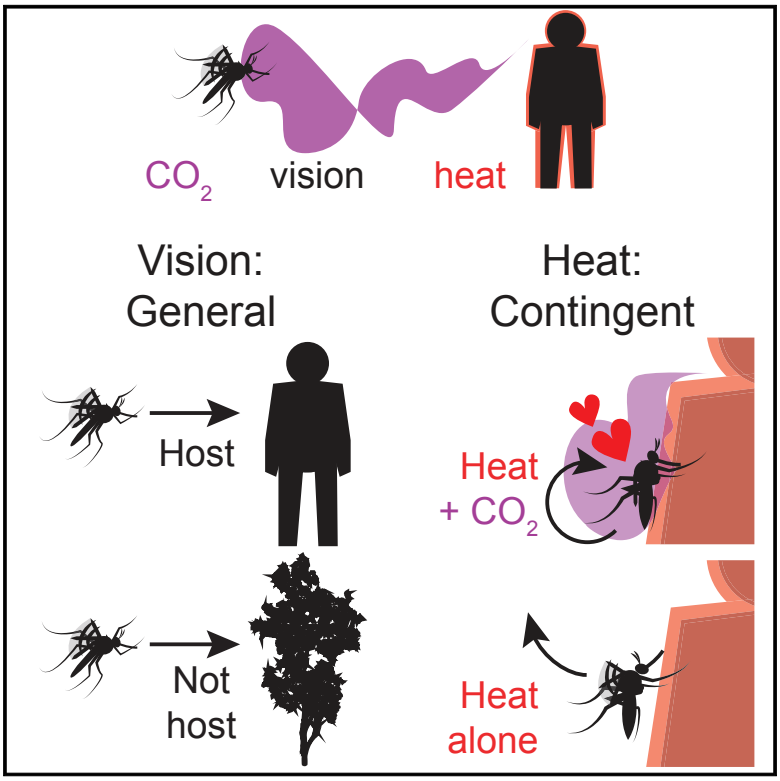

Authors

Molly Z. Liu, Leslie B. Vosshall

Correspondence

leslie.vosshall@rockefeller.edu

In Brief

Female *Aedes aegypti* mosquitoes are nature's human-seeking missiles, and they use multiple sensory modalities to hunt us. Liu and Vosshall study how CO_2 from breath, body heat, and visual cues contributes to host pursuit. They find that mosquito visual responses are unaffected by CO_2, but mosquitoes must sense CO_2 to unlock their attraction to heat.

Highlights

- Mosquito attraction to dark visual contrast is not contingent on other host cues
- Attractive visual cues enhance the attractiveness of warm stimuli
- Carbon dioxide contingently unlocks thermotaxis toward potential hosts

Liu & Vosshall, 2019, Current Biology *29*, 2250–2257
July 8, 2019
https://doi.org/10.1016/j.cub.2019.06.001

CellPress

CellPress

Current Biology
Report

General Visual and Contingent Thermal Cues Interact to Elicit Attraction in Female *Aedes aegypti* Mosquitoes

Molly Z. Liu[1] and Leslie B. Vosshall[1,2,3,4,*]
[1]Laboratory of Neurogenetics and Behavior, The Rockefeller University, New York, NY 10065, USA
[2]Howard Hughes Medical Institute, New York, NY 10065, USA
[3]Kavli Neural Systems Institute, New York, NY 10065, USA
[4]Lead Contact
*Correspondence: leslie.vosshall@rockefeller.edu
https://doi.org/10.1016/j.cub.2019.06.001

SUMMARY

Female *Aedes aegypti* mosquitoes use multiple sensory modalities to hunt human hosts and obtain a blood meal for egg production. Attractive cues include carbon dioxide (CO_2), a major component of exhaled breath [1, 2]; heat elevated above ambient temperature, signifying warm-blooded skin [3, 4]; and dark visual contrast [5, 6], proposed to bridge long-range olfactory and short-range thermal cues [7]. Any of these sensory cues in isolation is an incomplete signal of a human host, and so a mosquito must integrate multimodal sensory information before committing to approaching and biting a person [8]. Here, we study the interaction of visual cues, heat, and CO_2 to investigate the contributions of human-associated stimuli to host-seeking decisions. We show that tethered flying mosquitoes strongly orient toward dark visual contrast, regardless of CO_2 stimulation and internal host-seeking status. This suggests that attraction to visual contrast is general and not contingent on other host cues. In free-flight experiments with CO_2, adding a dark contrasting visual cue to a warmed surface enhanced attraction. Moderate warmth became more attractive to mosquitoes, and mosquitoes aggregated on the cue at all non-noxious temperatures. *Gr3* mutants, unable to detect CO_2, were lured to the visual cue at ambient temperatures but fled and did not return when the surface was warmed to host-like temperatures. This suggests that attraction to thermal cues is contingent on the presence of the additional sensory cue CO_2. Our results illustrate that mosquitoes integrate general attractive visual stimuli with context-dependent thermal stimuli to seek promising sites for blood feeding.

RESULTS AND DISCUSSION

Tethered Mosquito Visual Responses Are Not Altered by Host-Seeking State

We built a magnetic tether ("magnotether") to study orientation responses in flying mosquitoes to temporally and spatially controlled visual stimuli (Figure 1A; Video S1 [5, 9, 10]). Free rotation within the magnotether allows animals to control their own flight turns naturalistically, avoiding the confounds that arise from rigid-tether closed-loop experiments where the gains of visual feedback are arbitrarily chosen [11]. Because animals must be flying to be assayed in the magnotether, we focused solely on orientation in flight. In each trial, we showed an individually tethered animal a shape, such as a long dark stripe (Figure 1B), recorded the animal's orientation over time (Figure 1C), computed the offset between the stimulus and animal position (Figure 1D), and calculated the proportion of time spent with an offset within ±45° to obtain "fixation" (expected ~1.00 for attractive shapes; Figure 1E). As controls, we presented animals with trials where only a static background was shown ("blank") and computed offset and fixation relative to a randomly assigned fictive stimulus position (expected ~0.25; Figures 1F–1I).

To confirm that our magnotether accurately captured object responses, we presented female *Drosophila melanogaster* flies with simple dark shapes that had known response profiles (Figure S1A). Replicating previous results [12, 13], flies oriented strongly toward the long stripe, showed weak responses to the medium stripe, and avoided the small square (Figures S1B and S1C).

According to previous work in flies [14, 15] and mosquitoes [5], insects track odors more reliably in patterned visual environments. Because we were interested in odor-mediated modulation of visual responses, we presented the same simple shapes to flying female *Ae. aegypti* but on a patterned low-light background instead of the uniform background used for flies. This patterned background also allowed us to present both dark and bright shapes in the same environment. Because we could not detect any statistical effect of age on the fixation responses of our 5–16 days post-eclosion animals (data not shown), we pooled results from all age groups for analysis.

Previous reports indicated that loosely tethered mosquitoes orient toward long dark stripes, but not toward long bright stripes

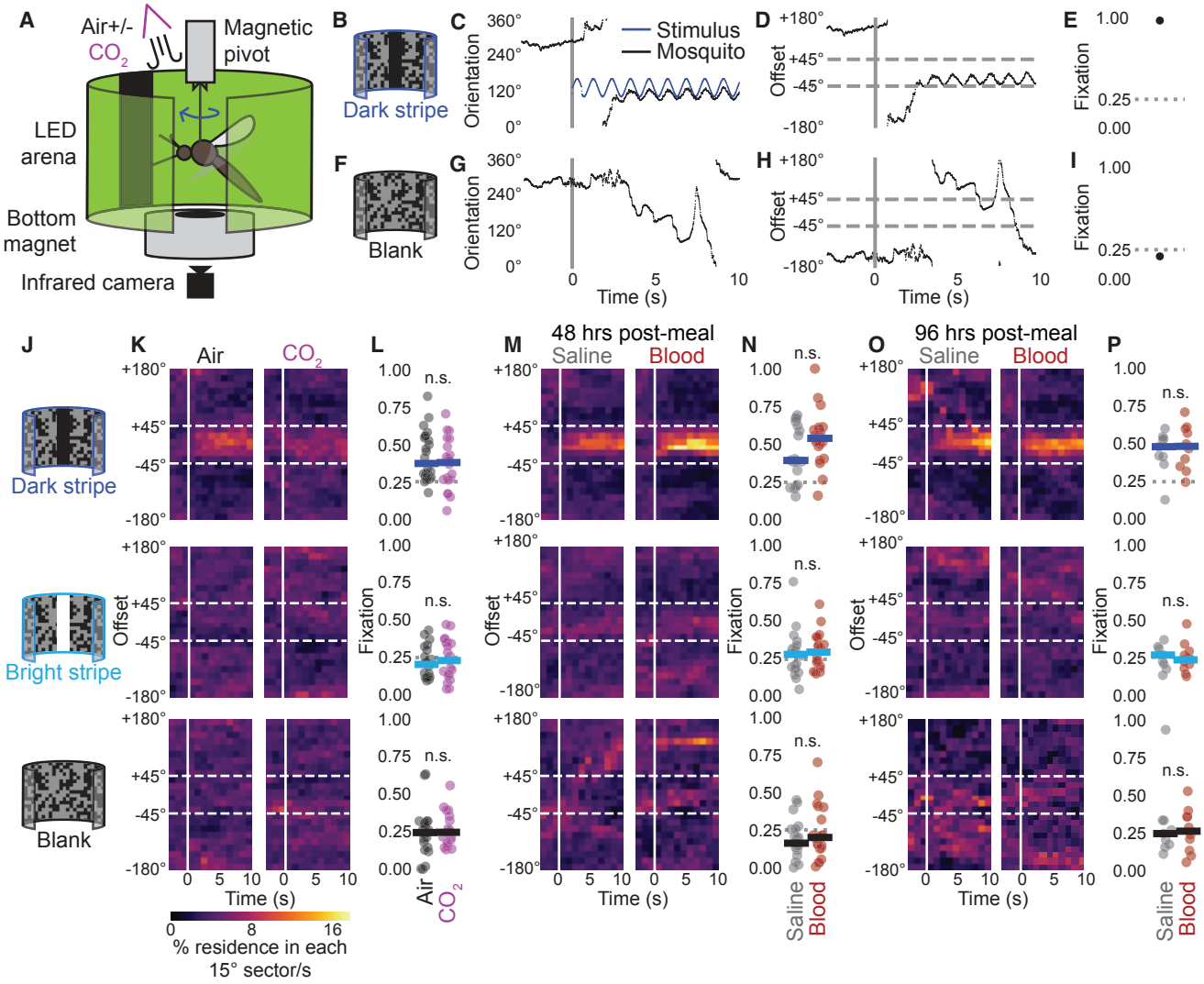

Figure 1. Mosquito Visual Responses Are Not Influenced by Host-Seeking Status

(A) Magnotether schematic (not to scale).

(B–I) Example magnotether traces from dark stripe (B–E) or blank (F–I) trials.

(J) Magnotether stimuli.

(K, M, and O) Heatmaps of offset, parsed by shape of stimulus, from mosquitoes tested in air (n = 24 dark and blank; n = 20 bright) or CO_2 (n = 20, dark and blank; n = 21, bright; K); 48 h post-meal, saline (n = 20) and blood (n = 20; M); and 96 h post-meal, saline (n = 9) and blood (n = 10; O). Each trial corresponds to a single female.

(L, N, and P) Fixation parsed by shape in J comparing mosquitoes tested in air or CO_2 (L), 48 hr post-meal, saline, and blood (N), and 96 hr post-meal, saline, and blood (n = 10) (P). Mann-Whitney U test with Bonferroni correction.

Dashed lines: bounds used to calculate fixation. Solid lines: onset of visual stimulus. Dotted lines: expected fixation for uniform orientation. See also Figures S1 and S2 and Video S1.

or blank control stimuli [5]. We investigated whether those visual responses were altered by elevated CO_2 (Figure 1J). Both non-directionally [8] and as a plume [1], CO_2 is a potent signature of host breath that amplifies responses to other host cues. In the magnotether, we applied non-directional pulses of CO_2, previously shown to increase mosquito responses to human odor and heat [8].

However, in contrast to a previous report [7], we could not detect changes in the visual orientation responses of our tethered mosquitoes after contact with increased levels of CO_2 for any shape tested (Figures 1K, 1L, and S2). We suggest that this apparent conflict is resolved if mosquitoes are attracted to the presented dark contrast while flying, regardless of CO_2 activation. Instead of CO_2 potentiating visual attraction, as previously proposed [7], CO_2 plumes may cause freely moving mosquitoes to increase approach to visual stimuli by potently activating and lengthening their flight. Without activation by CO_2, mosquitoes in a free flight arena initiate fewer flights and fly shorter distances [8], and so they may not approach visual stimuli. Conversely, tethered mosquitoes are always flying, and

so introducing CO_2 does not affect their propensity to fly toward dark contrast. Our results are replicated in a recent study [16] in which rigidly tethered mosquitoes track a dark stripe and dark square of analogous size to those studied here. In that study, although an effect was found with a small square, adding a plume of CO_2 did not significantly change fidelity of tracking to these larger shapes. We thus propose that elevated CO_2 may increase visual attraction in freely moving mosquitoes by increasing flight probability, not by changing the attractiveness of the visual stimulus.

Attraction to host cues is also modulated by internal state. When a female mosquito ingests a blood meal, her previously strong attraction to host cues is suppressed until she lays eggs [17]. Conversely, mosquitoes fed saline continue to be attracted to hosts. We compared visual orientation behaviors of mosquitoes after ingestion of blood or saline and did not detect a difference in visual orientation for any shape tested (Figures 1M–1P and S2).

To investigate the relationship between fixation and shape height, we pooled data from statistically indistinguishable trials (Figures S1D–S1I). Confirming previous results that indicated that mosquitoes pay attention to contrast polarity [5, 7], we found that dark stripes were consistently more attractive than blank controls, whereas bright shapes were indistinguishable from blank controls. Although dark square responses were always indistinguishable from those of dark stripes, they were also indistinguishable from blank controls except 48 h post-meal. Because mosquitoes 48 h after a saline meal behave like non-fed mosquitoes in other assays [18], we speculate that this is due to behavioral variation in the assay. From our data, we are unable to conclude whether mosquitoes exhibit strong height-based tuning to their fixation responses, but we see clear evidence that mosquitoes show general, non-contingent attraction to large areas of dark visual contrast. We suggest that mosquitoes use dark visual contrast as signals of potential landing sites, as has been proposed for *Drosophila* [19].

Thermotaxis Is Enhanced by Co-presentation of a Visual Cue

Given that responses to visual cues in the magnotether are not modulated by CO_2 or blood feeding, we asked a reciprocal question: how do visual cues affect mosquito responses to a signature host cue, such as human skin temperature? To test this, we adapted a previously described free flight thermotaxis assay [4] that measures mosquito occupancy on a temperature-controlled Peltier in the presence of CO_2. We modified the Peltier by affixing a 2-cm black circle (“dot”) to its center (Figure 2A). We chose this visual stimulus because it was previously shown to attract mosquitoes and be modulated by heat in free flight [7]. We tracked the two-dimensional location of mosquitoes while setting the internal temperature of the Peltier to various temperatures (Figure 2B). The dot did not present a detectably different thermal signature from the rest of the Peltier (Figure 2C), meaning that any differences in occupancy should be due to visual features of the dot. Because heat dissipates rapidly over air, a landed mosquito experiences temperatures lower than those recorded from the Peltier surface, hereafter “Peltier temperature,” as verified by air temperatures measured at a mosquito’s estimated center of mass when landed on the Peltier (Figure 2D).

We presented a heat ramp with either a dot or blank control to groups of 45–50 female mosquitoes, co-presented with pulses of CO_2 (Figure 2E). Consistent with a previous study [4], mosquito occupancy on the Peltier increased as the temperature heated to 28.5°C–50°C and then decreased as it heated to 55°C–60°C (Figure 2F). Air temperature measurements at a mosquito body’s estimated landed distance during these attractive temperatures (27.9°C–32.2°C; Figure 2D) approximated the temperature range of human skin, 29°C–35°C [20].

We saw two striking differences when the dot was present. First, mosquitoes occupied the unheated Peltier at high rates when it was set to ambient temperature (26°C), including between heat bouts and before pulses of CO_2 (Figure 2G). This is consistent with our finding that tethered mosquitoes are attracted to dark contrast independent of elevated CO_2 (Figures 1 and S2), as well as previously published findings showing that freely flying mosquitoes approached small black dots [7]. Mosquitoes also took off from the dot at ambient temperature after a pulse of CO_2, consistent with findings that CO_2 promotes take-off [8]. Second, the dot enhanced total levels of mosquito occupancy on the Peltier at temperatures warmer than ambient but cooler than human skin (Peltier temperatures: 28.5°C–31°C; Figure 2H).

To examine the effect of the dot more closely, we compared mosquito locations with and without the visual cue during thermotaxis (Figure 2I). With the visually blank Peltier, mosquitoes spread themselves evenly across the warm Peltier, with a slight bias toward the bottom edge. However, when the dot was present, mosquitoes aggregated on and around the dot at all non-noxious temperatures (Peltier temperatures: 26°C–50°C; Figure 2J). The same results were obtained when we randomized the order of the Peltier temperatures, showing that these effects do not depend on past history of thermal presentation (Figure S3). These results replicate and expand upon a previous finding that visual contrast enhances heat seeking [7].We have begun to elucidate the precise mechanisms by which this enhancement occurs by showing that moderate warmth becomes more attractive to mosquitoes when visually marked, and mosquitoes aggregate on areas of high contrast at all attractive temperatures.

Occupancy on Host-like Temperatures Is Contingent on Sensation of Elevated CO_2

Finally, the general attractiveness of the visual cue allowed us to investigate the role of CO_2 in host seeking. Previous reports showed that mosquito thermal attraction is enhanced by CO_2 [3, 8, 21], which could be through at least two non-mutually exclusive mechanisms. First, CO_2 could increase the propensity of mosquitoes to take off and remain in flight, which would increase their probability of coming close enough to a surface to sense its heat. Second, CO_2 could alter the thermal preferences of mosquitoes so that they become attracted to temperatures they would ordinarily ignore or avoid. To test these possibilities, we used the dot to lure mosquitoes to the unheated Peltier (Figure 2G). Although previous assays have examined approach to heated objects [4, 7], we are here able to examine the responses of landed mosquitoes to heat. If mosquitoes are always attracted to host-like temperatures, then they should continue occupying a marked surface upon heating, regardless of CO_2 sensation.

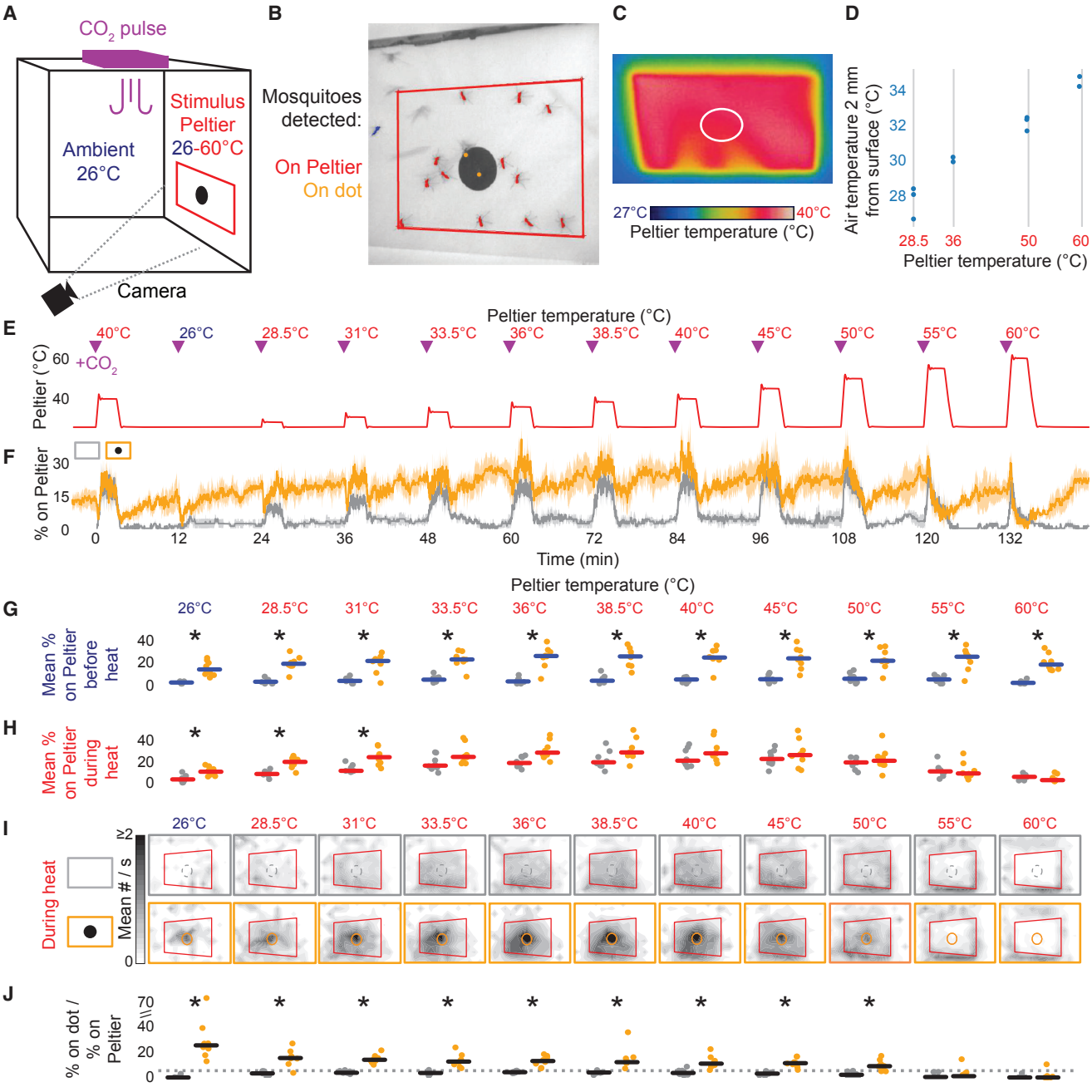

Figure 2. Visual Cue Enhances Mosquito Thermotaxis to Moderate Heat

(A) Schematic of heat-seeking assay with 2-cm-diameter black dot as visual cue.

(B) Camera image, showing mosquitoes on Peltier (red outline) sampled at 1 Hz.

(C) Thermal image of the Peltier set to 40°C. White outline: boundary of black dot.

(D) Median air temperature 2 mm from surface graphed as a function of Peltier temperature during 90–180 s of heat bouts set to 28.5°C, 36°C, 50°C, and 60°C (vertical gray lines); n = 3.

(E) Peltier temperature. CO_2 was pulsed in for 20 s at onset of each heat bout (purple triangle).

(F) Median % of mosquitoes on Peltier over entire experiment ± median absolute deviation, blank (gray, n = 8) or visual cue (orange, n = 8). Each trial involved 45–50 mosquitoes.

(G, H, and J) Median percent of mosquitoes on the Peltier 90–0 s before onset of heat ("before heat"; G), 90–180 s after onset of heat ("during heat"; H), and on the area of the dot during heat (J), normalized by median % of mosquitoes anywhere on the Peltier ("on dot"). Dotted line in (J) indicates expected value from a uniform spatial distribution. *$p < 0.05$; Mann-Whitney U test with Bonferroni correction.

(I) Heatmaps showing mean mosquito occupancy on the Peltier (red outline) and surrounding area with blank (gray) or visual cue (orange) during seconds 90–180 of heat.

See also Figure S3.

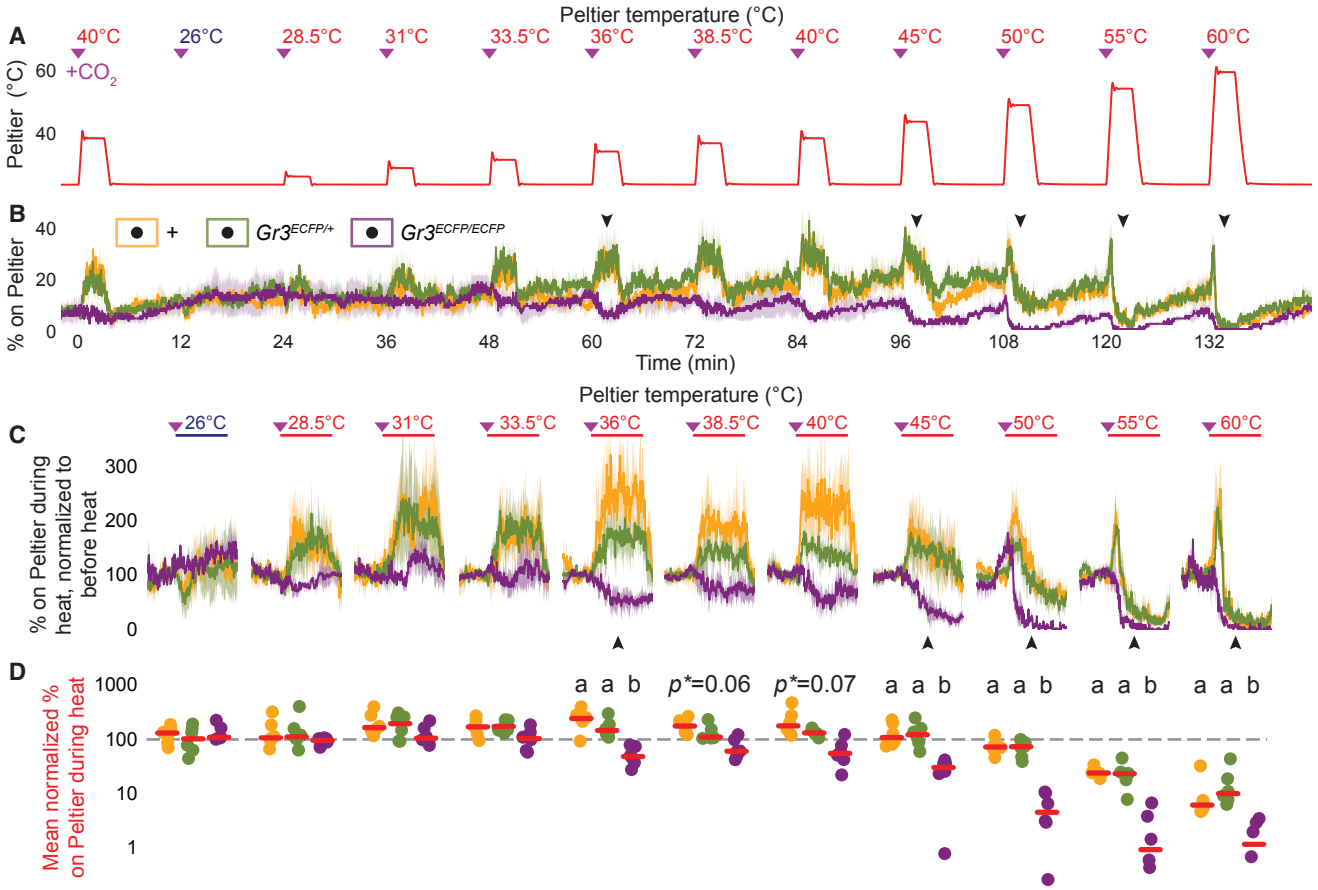

Figure 3. Mosquito Thermotaxis Requires CO_2 Sensation

(A) Peltier temperature. CO_2 was pulsed for 20 s at onset of each heat bout (purple triangle).

(B) Median % ± median absolute deviation of mosquitoes on Peltier marked with a visual cue. Genotypes: $Gr3^{+/+}$ (orange, n = 6), $Gr3^{ECFP/+}$ (green, n = 6), and $Gr3^{ECFP/ECFP}$ (purple, n = 6) are shown.

(C) Median % ± median absolute deviation of residence on Peltier over time, normalized to mean residence before heat. Purple triangle: CO_2 pulse. Red horizontal line: heat on.

(D) Median % of mosquitoes on the Peltier during heat, normalized as in (C), and plotted on a log10 scale to highlight deviation from 100% (dotted line). Different letters: significantly distinct data ($p < 0.05$), assessed with Kruskal-Wallis test with Bonferroni correction, and then post hoc Mann-Whitney U test with Bonferroni correction.

See also Figure S4.

Conversely, if we only see thermal occupancy coincident with sensed CO_2 elevation, then CO_2 must be shifting mosquito thermal preferences.

CO_2 is a pervasive and naturally occurring stimulus that is difficult to remove from behavioral assays. As an alternative approach, we used $Gr3^{ECFP/ECFP}$ mosquitoes, which lack a functional CO_2 receptor and cannot detect CO_2 [8], to test responses to a heat ramp (Figure 3A) with a dot-marked Peltier. Regardless of their ability to sense CO_2, mosquitoes accumulated on the Peltier between heat bouts (Figure 3B), replicating our observation that CO_2 does not alter mosquito general visual preferences in the magnotether assay (Figures 1K and 1L).

However, whereas wild-type and $Gr3^{ECFP/+}$ heterozygous mosquitoes increased Peltier occupancy with increasing temperatures, $Gr3^{ECFP/ECFP}$ mutant mosquitoes left the Peltier when it was heated to host-like temperatures (Figures 3C and 3D). We observed the same decrease in occupancy in wild-type mosquitoes tested without CO_2 pulses (Figure S4), indicating that this effect is likely a general consequence of CO_2 sensation. We speculate that CO_2 shifts mosquito thermal preferences in a manner independent of visual stimuli, causing mosquitoes to pursue elevated heat only when they have corroborating evidence that the heat comes from a breathing host.

Sensation of Elevated CO_2 Drives Mosquitoes to Repeatedly Land on Heat

CO_2 could act to increase occupancy on host-like temperatures by causing mosquitoes to dwell on heat longer or to land more frequently on heat. To examine how these rates changed, we manually tracked landings on and take-offs from the Peltier set to 36°C. This temperature in combination with CO_2 attracts wild-type and $Gr3^{ECFP/+}$ heterozygous mosquitoes but repels

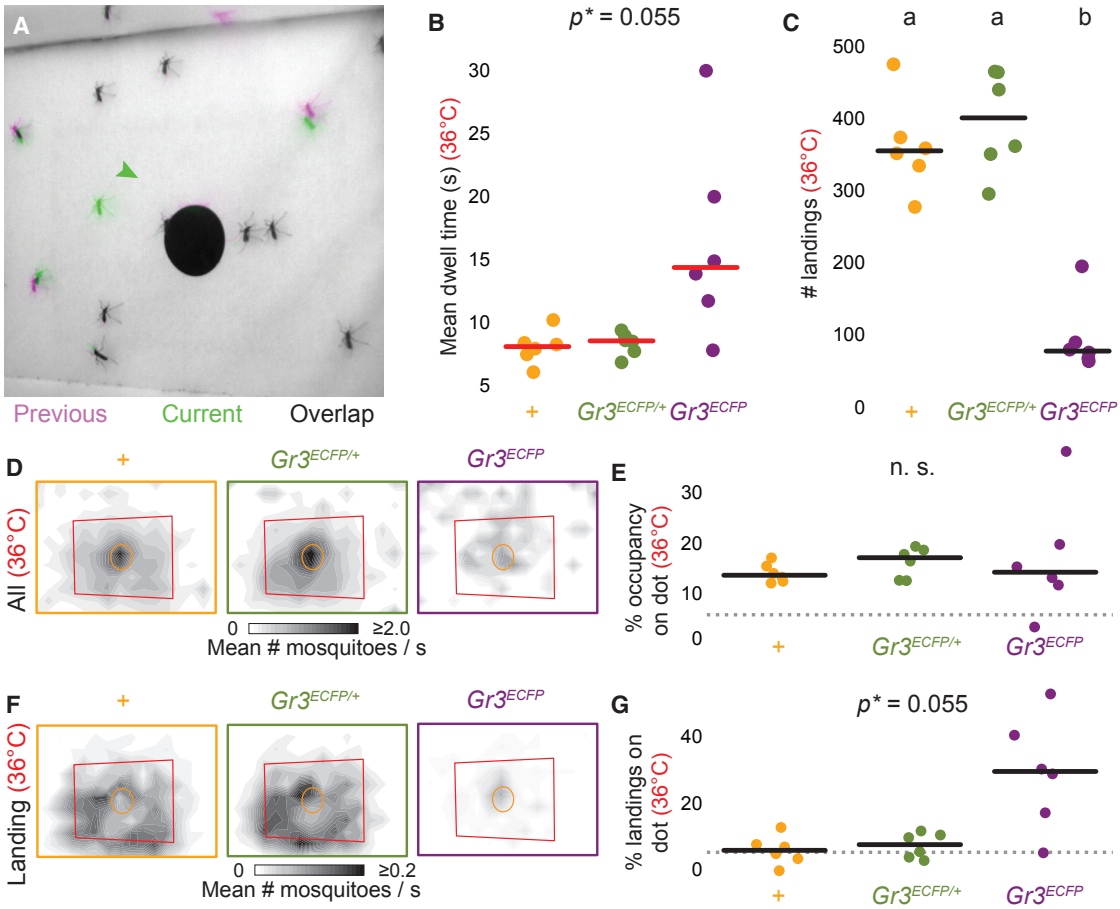

Figure 4. CO_2 Sensation Induces Repeated Return to Heat

(A) Example superimposed consecutive frames from 36°C heat bout in experiments shown in Figure 3. Green arrowhead: landing event.

(B and C) Mean dwell time (B) and number of landings (C) of $Gr3^{+/+}$ (orange, n = 6), $Gr3^{ECFP/+}$ (green, n = 6), and $Gr3^{ECFP/ECFP}$ (purple, n = 6) on Peltier wall during 36°C heat.

(D and F) Heatmaps showing total mosquito occupancy (D) and landing events (F) or total mosquito occupancy on the Peltier (red outline) and surrounding area during entire 180-s 36°C heat bout. Visual cue is marked in orange.

(E) Median % occupancy on the dot, normalized by % occupancy on the entire area of the Peltier. Dotted line: expected value from a uniform spatial distribution.

(G) Median landing events on the dot as a percentage of the number of landing events on the entire area of the Peltier. Dotted line: expected value from a uniform spatial distribution.

Different letters in (B), (C), (E), and (G): significantly distinct data ($p < 0.05$), assessed with Kruskal-Wallis test with Bonferroni correction, and then post hoc Mann-Whitney U test with Bonferroni correction.

$Gr3^{ECFP/ECFP}$ mosquitoes (Figure 4A), allowing us to compute a population mean dwell time on heat using times of landings and take-offs.

Interestingly, wild-type and $Gr3^{ECFP/+}$ heterozygous mosquitoes did not dwell longer on heat than $Gr3^{ECFP/ECFP}$ mosquitoes (Figure 4B), perhaps because CO_2-sensitive mosquitoes have been activated by CO_2 and may be hyperactively exploring. Unlike CO_2-sensitive mosquitoes, CO_2-insensitive mosquitoes do not increase their general motor activity after CO_2 pulses [8]. This suggests that 36°C heat alone is an aversive cue for a landed mosquito, replicating previous findings in which mosquitoes walking on a thermal gradient avoided temperatures above 30°C [4, 22]. Instead, the increase in occupancy primarily comes from increased landing of CO_2-sensitive mosquitoes on host-like temperatures (Figure 4C). Furthermore, in CO_2-sensitive mosquitoes, the number of landings was five to ten times greater than the number of mosquitoes, indicating that individual mosquitoes must be landing and taking off multiple times. Mosquito attraction to host-like temperatures is thus contingent on the sensation of elevated CO_2, which drives mosquitoes to repeatedly return to the thermal stimulus.

In addition to changing rates of landing, we asked whether CO_2 sensation changed the spatial pattern of mosquito landings. Similar to previous results (Figures 2I and 2J), mosquitoes aggregated preferentially on the dot at 36°C. This effect did not vary by genotype (Figures 4D and 4E), suggesting that it does not depend on CO_2 sensation. However, location of landings alone appeared somewhat different, with CO_2-sensitive wild-type and $Gr3^{ECFP/+}$ heterozygous mosquitoes landing across the Peltier, consistent with a uniform

distribution on heat, and $Gr3^{ECFP/ECFP}$ mutants tending to land preferentially on the dot (Figures 4F and 4G). We speculate that, without elevated CO_2, mosquitoes primarily use visual cues to land, and CO_2 sensation allows mosquitoes to also land on thermal cues.

Conclusions

In this study, we show that both visual contrast and heat contribute to mosquito attraction. Whereas visual contrast is generally attractive even outside the context of host seeking, attraction to heat is contingent upon co-presentation of the chemosensory host-cue CO_2. We speculate that this attraction to visual contrast in flight may be adaptive because flying is an energetically expensive activity [23], so finding a dark landing location may provide general respite and camouflage. However, residence on high heat brings with it threats of damage and desiccation. Indeed, mosquitoes die after 30-min exposures to air temperatures above 42°C [24]. Mosquitoes may balance this thermal threat of heat against the beneficial use of heat as a potent signature of warm-blooded hosts by only thermotaxing when they detect other reliable host cues, such as CO_2.

All animals must dynamically weigh their sensory landscape to make decisions. Studies of *Drosophila* species have described the serial sensory modules that underlie behaviors from courtship [25–27] to flight navigation [28, 29]. Here, we show that *Ae. aegypti* mosquitoes use serial sensory modules in host seeking. They fly toward visual contrast and then sense CO_2 to unlock thermotaxis toward potential hosts. Mosquitoes across the Culicidae family display an impressive variety of host choices, from mammals to cold-blooded frogs [30] to annelids [31], and the algorithms they use to weigh sensory host cues likely vary just as much. Our results illustrate how such weighting is performed in one species, providing a first glimpse into how general and contingent cues are integrated to produce host-seeking behavior in mosquitoes. With the rapid development of genetic and neuroscience tools in mosquitoes [32–35], we are poised to uncover the neuronal mechanisms underlying multimodal integration in these charismatic and deadly insects.

STAR★METHODS

Detailed methods are provided in the online version of this paper and include the following:

- KEY RESOURCES TABLE
- LEAD CONTACT AND MATERIALS AVAILABILITY
- EXPERIMENTAL MODEL AND SUBJECT DETAILS
  - Fly Rearing and Maintenance
  - Mosquito Rearing and Maintenance
  - Gr3 Mutant Strain
- METHOD DETAILS
  - Fly Magnetic Tethering
  - Mosquito Magnetic Tethering
  - Glytube Blood-Meal Feeding
  - Heat-Seeking Assay
- QUANTIFICATION AND STATISTICAL ANALYSIS
- DATA AND CODE AVAILABILITY

SUPPLEMENTAL INFORMATION

Supplemental Information can be found online at https://doi.org/10.1016/j.cub.2019.06.001.

ACKNOWLEDGMENTS

We thank Román Corfas, Caroline Kittredge Faustine, Lisa Fenk, Kaela Mei-Shing Garvin, Itzel Ishida, Cheng Lyu, Gaby Maimon, Vanessa Ruta, Cameron Toy, Waring Trible, and members of the Vosshall lab for discussion and comments on the manuscript; Lisa Fenk, Jonathan Green, Jonathan Hirokawa, and Gaby Maimon for magnotether discussions, equipment, and technical advice; Takeshi Morita for technical advice on the heat-seeking experiments; and Gloria Gordon for expert mosquito rearing. L.B.V. is an investigator of the Howard Hughes Medical Institute. The ORCIDs for the authors are 0000-0002-1593-9964 (M.Z.L.) and 0000-0002-6060-8099 (L.B.V.).

AUTHOR CONTRIBUTIONS

Supervision and Funding Acquisition, L.B.V.; Investigation, M.Z.L.; Conceptualization, Methodology, and Writing, M.Z.L. and L.B.V.

DECLARATION OF INTERESTS

The authors declare no competing interests.

Received: January 6, 2019
Revised: April 29, 2019
Accepted: June 3, 2019
Published: June 27, 2019

REFERENCES

1. Dekker, T., Geier, M., and Cardé, R.T. (2005). Carbon dioxide instantly sensitizes female yellow fever mosquitoes to human skin odours. J. Exp. Biol. *208*, 2963–2972.
2. Majeed, S., Hill, S.R., and Ignell, R. (2014). Impact of elevated CO2 background levels on the host-seeking behaviour of *Aedes aegypti*. J. Exp. Biol. *217*, 598–604.
3. Burgess, L. (1959). Probing behaviour of *Aedes ægypti* (L.) in response to heat and moisture. Nature *184*, 1968–1969.
4. Corfas, R.A., and Vosshall, L.B. (2015). The cation channel TRPA1 tunes mosquito thermotaxis to host temperatures. eLife *4*, e11750.
5. Kennedy, J.S. (1940). The visual responses of flying mosquitoes. J. Zool., A. *109*, 221–242.
6. Brown, A.W.A. (1951). Studies of the responses of the female *Aëdes* mosquito. Part IV. Field experiments on Canadian species. Bull. Entomol. Res. *42*, 575–582.
7. van Breugel, F., Riffell, J., Fairhall, A., and Dickinson, M.H. (2015). Mosquitoes use vision to associate odor plumes with thermal targets. Curr. Biol. *25*, 2123–2129.
8. McMeniman, C.J., Corfas, R.A., Matthews, B.J., Ritchie, S.A., and Vosshall, L.B. (2014). Multimodal integration of carbon dioxide and other sensory cues drives mosquito attraction to humans. Cell *156*, 1060–1071.
9. Bender, J.A., and Dickinson, M.H. (2006). Visual stimulation of saccades in magnetically tethered *Drosophila*. J. Exp. Biol. *209*, 3170–3182.
10. Reiser, M.B., and Dickinson, M.H. (2008). A modular display system for insect behavioral neuroscience. J. Neurosci. Methods *167*, 127–139.
11. Fenk, L.M., Poehlmann, A., and Straw, A.D. (2014). Asymmetric processing of visual motion for simultaneous object and background responses. Curr. Biol. *24*, 2913–2919.
12. Theobald, J.C., Duistermars, B.J., Ringach, D.L., and Frye, M.A. (2008). Flies see second-order motion. Curr. Biol. *18*, R464–R465.
13. Mongeau, J.M., and Frye, M.A. (2017). *Drosophila* spatiotemporally integrates visual signals to control saccades. Curr. Biol. *27*, 2901–2914.e2.

14. Frye, M.A., Tarsitano, M., and Dickinson, M.H. (2003). Odor localization requires visual feedback during free flight in *Drosophila melanogaster*. J. Exp. Biol. *206*, 843–855.

15. Dickinson, M.H. (2014). Death Valley, *Drosophila*, and the Devonian toolkit. Annu. Rev. Entomol. *59*, 51–72.

16. Vinauger, C., Van Breugel, F., Locke, L.T., Tobin, K.K.S., Dickinson, M.H., Fairhall, A., Akbari, O.S., and Riffell, J.A. (2019). Visual-olfactory integration in the human disease vector mosquito, *Aedes aegypti*. bioRxiv. https://doi.org/10.1101/512996.

17. Klowden, M.J. (1981). Initiation and termination of host-seeking inhibition in *Aedes aegypti* during oöcyte maturation. J. Insect Physiol. *27*, 799–803.

18. Duvall, L.B., Ramos-Espiritu, L., Barsoum, K.E., Glickman, J.F., and Vosshall, L.B. (2019). Small-molecule agonists of *Ae. aegypti* neuropeptide Y receptor block mosquito biting. Cell *176*, 687–701.e5.

19. Maimon, G., Straw, A.D., and Dickinson, M.H. (2008). A simple vision-based algorithm for decision making in flying *Drosophila*. Curr. Biol. *18*, 464–470.

20. Yao, Y., Lian, Z., Liu, W., and Shen, Q. (2008). Experimental study on physiological responses and thermal comfort under various ambient temperatures. Physiol. Behav. *93*, 310–321.

21. Kröber, T., Kessler, S., Frei, J., Bourquin, M., and Guerin, P.M. (2010). An in vitro assay for testing mosquito repellents employing a warm body and carbon dioxide as a behavioral activator. J. Am. Mosq. Control Assoc. *26*, 381–386.

22. Blanford, S., Read, A.F., and Thomas, M.B. (2009). Thermal behaviour of *Anopheles stephensi* in response to infection with malaria and fungal entomopathogens. Malar. J. *8*, 72.

23. Reinhold, K. (1999). Energetically costly behaviour and the evolution of resting metabolic rate in insects. Funct. Ecol. *13*, 217–224.

24. Eisen, L., Monaghan, A.J., Lozano-Fuentes, S., Steinhoff, D.F., Hayden, M.H., and Bieringer, P.E. (2014). The impact of temperature on the bionomics of *Aedes* (Stegomyia) *aegypti*, with special reference to the cool geographic range margins. J. Med. Entomol. *51*, 496–516.

25. Agrawal, S., Safarik, S., and Dickinson, M. (2014). The relative roles of vision and chemosensation in mate recognition of *Drosophila melanogaster*. J. Exp. Biol. *217*, 2796–2805.

26. Clowney, E.J., Iguchi, S., Bussell, J.J., Scheer, E., and Ruta, V. (2015). Multimodal chemosensory circuits controlling male courtship in *Drosophila*. Neuron *87*, 1036–1049.

27. Coen, P., Xie, M., Clemens, J., and Murthy, M. (2016). Sensorimotor transformations underlying variability in song intensity during *Drosophila* courtship. Neuron *89*, 629–644.

28. van Breugel, F., and Dickinson, M.H. (2014). Plume-tracking behavior of flying *Drosophila* emerges from a set of distinct sensory-motor reflexes. Curr. Biol. *24*, 274–286.

29. Currier, T.A., and Nagel, K.I. (2018). Multisensory control of orientation in tethered flying *Drosophila*. Curr. Biol. *28*, 3533–3546.e6.

30. Bartlett-Healy, K., Crans, W.J., and Gaugler, R. (2008). Phonotaxis to amphibian vocalizations in *Culex territans* (Diptera: Culicidae). Ann. Entomol. Soc. Am. *101*, 95–103.

31. Reeves, L.E., Holderman, C.J., Blosser, E.M., Gillett-Kaufman, J.L., Kawahara, A.Y., Kaufman, P.E., and Burkett-Cadena, N.D. (2018). Identification of Uranotaenia sapphirina as a specialist of annelids broadens known mosquito host use patterns. Commun. Biol. *1*, 92.

32. Kokoza, V.A., and Raikhel, A.S. (2011). Targeted gene expression in the transgenic *Aedes aegypti* using the binary Gal4-UAS system. Insect Biochem. Mol. Biol. *41*, 637–644.

33. Riabinina, O., Task, D., Marr, E., Lin, C.C., Alford, R., O'Brochta, D.A., and Potter, C.J. (2016). Organization of olfactory centres in the malaria mosquito *Anopheles gambiae*. Nat. Commun. *7*, 13010.

34. Ruzzante, L., Reijnders, M.J.M.F., and Waterhouse, R.M. (2019). Of genes and genomes: mosquito evolution and diversity. Trends Parasitol. *35*, 32–51.

35. Matthews, B.J., Dudchenko, O., Kingan, S.B., Koren, S., Antoshechkin, I., Crawford, J.E., Glassford, W.J., Herre, M., Redmond, S.N., Rose, N.H., et al. (2018). Improved reference genome of *Aedes aegypti* informs arbovirus vector control. Nature *563*, 501–507.

36. Straw, A.D., and Dickinson, M.H. (2009). Motmot, an open-source toolkit for realtime video acquisition and analysis. Source Code Biol. Med. *4*, 5.

37. DeGennaro, M., McBride, C.S., Seeholzer, L., Nakagawa, T., Dennis, E.J., Goldman, C., Jasinskiene, N., James, A.A., and Vosshall, L.B. (2013). *orco* mutant mosquitoes lose strong preference for humans and are not repelled by volatile DEET. Nature *498*, 487–491.

38. Ferris, B.D., Green, J., and Maimon, G. (2018). Abolishment of spontaneous flight turns in visually responsive *Drosophila*. Curr. Biol. *28*, 170–180.e5.

39. Costa-da-Silva, A.L., Navarrete, F.R., Salvador, F.S., Karina-Costa, M., Ioshino, R.S., Azevedo, D.S., Rocha, D.R., Romano, C.M., and Capurro, M.L. (2013). Glytube: a conical tube and parafilm M-based method as a simplified device to artificially blood-feed the dengue vector mosquito, *Aedes aegypti*. PLoS ONE *8*, e53816.

40. Leys, C., Ley, C., Klein, O., Bernard, P., and Licata, L. (2013). Detecting outliers: do not use standard deviation around the mean, use absolute deviation around the median. J. Exp. Soc. Psychol. *49*, 764–766.

41. Pham-Gia, T., and Hung, T.L. (2001). The mean and median absolute deviations. Math. Comput. Model. *34*, 921–936.

STAR★METHODS

KEY RESOURCES TABLE

REAGENT or RESOURCE	SOURCE	IDENTIFIER
Deposited Data		
Raw and analyzed data	This paper	https://github.com/VosshallLab/LiuVosshall2019
Experimental Models: Organisms/Strains		
Drosophila melanogaster (isoD strain)	Maimon lab	N/A
Aedes aegypti (Orlando strain)	Vosshall lab	N/A
Aedes aegypti ($Gr3^{ECFP/ECFP}$ mutant)	[8]	https://doi.org/10.1016/j.cell.2013.12.044
Software and Algorithms		
Motmot toolkit (FView, FlyTrax)	[36]	https://doi.org/10.1186/1751-0473-4-5
Python Programming Language	Python Software Foundation	RRID: SCR_008394
SciPy	http://SciPy.org	RRID: SCR_008058
MATLAB	MathWorks	RRID: SCR_001622
Other		
Processing scripts for data	This paper	https://github.com/VosshallLab/LiuVosshall2019

LEAD CONTACT AND MATERIALS AVAILABILITY

Further information and requests for reagents should be directed to and will be fulfilled by the Lead Contact, Leslie Vosshall (leslie.vosshall@rockefeller.edu).

EXPERIMENTAL MODEL AND SUBJECT DETAILS

Fly Rearing and Maintenance

Drosophila melanogaster wild-type laboratory strains (isoD) were maintained and reared with 25°C, with a photoperiod of 12 hr light:12 hr dark on standard corn-meal agar. Flies were sexed and sorted under cold anesthesia (4°C).

Mosquito Rearing and Maintenance

Aedes aegypti wild-type laboratory strains (Orlando) and mutant strains were maintained and reared at 25-28°C, 70%–80% relative humidity with a photoperiod of 14 hr light:10 hr dark (lights on at 7 a.m.) as previously described [37]. Briefly, eggs were hatched in deoxygenated, deionized water with powdered Tetramin fish food and larvae were fed Tetramin tablets (Tetra) until pupation. Adult mosquitoes were housed with siblings in BugDorm-1 (Bugdorm) cages and provided constant access to 10% sucrose. Adult females were blood-fed on mice for stock maintenance and blood-fed on human subjects for generation of the $Gr3^{ECFP/ECFP}$ and $Gr3^{ECFP/+}$ mosquitoes used in experiments. Blood-feeding procedures with live mice and humans were approved and monitored by The Rockefeller University Institutional Animal Care and Use Committee and Institutional Review Board, protocols 15772 and LVO-0652, respectively. Human subjects gave their written informed consent to participate.

Gr3 Mutant Strain

$Gr3^{ECFP/ECFP}$ mutants used in this study carry a broadly expressed ECFP marker inserted into the *Gr3* locus as described [8]. $Gr3^{ECFP/+}$ heterozygotes were the offspring of $Gr3^{ECFP/ECFP}$ males and wild-type (Orlando) females.

METHOD DETAILS

Fly Magnetic Tethering

For experiments in Figure S1, flies were magnetically tethered as described [38]. Female flies were collected 1-4 days after eclosion, anesthetized on a Peltier stage at ~4°C for 15-30 min, and attached by the dorsal part of their prothorax to a steel pin (0.10 mm Minutiens cut to 4-6 mm height, Austerlitz) using blue-light activated glue (Bondic, Canada). For 1-4 hr after tethering, flies recovered in a dark, humid chamber while holding small squares of tissue paper.

Flies were then suspended in a vertically-aligned magnetic field in the center of a cylindrical LED display (570 nm, IORodeo) covering 360 in azimuth and 94 in elevation with each pixel subtending ~3.75°. LEDs were controlled using PControl in MATLAB

[10]. In each experimental bout, flies were exposed to up to six types of visual stimuli composed of LEDs either off (“dark”) or maximally on (luminance 70. cd m^{-2}, “bright”), based on previous work [19]: black horizontally centered rectangles 94° tall x 15° wide (“long stripe”), 46x15° (“medium stripe”), and 15x15° (“square”); a uniform bright field (“blank”); a square wave grating composed of 24 alternating bright and dark 15° stripes; and a randomly composed pattern of shuffled dark and bright pixels (“contour”), not analyzed here. The long stripe, medium stripe, square, blank, and contour were randomly presented in 15 s trials, with every 10-16 trials interspersed by a moving 15 s square wave grating stimulus. Each trial presented the shape at a random position on the arena, moving in a sinusoid of peak-to-peak amplitude 60° and frequency randomly chosen from 0, 0.1, 0.2, 0.5, 1.0, 2.0, 4.0, 6.0, or 8.0 Hz. Flies that failed to follow the direction of wide-field motion or failed to sustain flight were discarded.

Flies were lit from below with IR LEDs (850 nm, DigiKey) and video was captured with an infrared-sensitive camera (AVT-GE680) triggered externally, recording frames (320x240 pixels) at 200 Hz. Fly body orientation was extracted from camera images in real time using FView and FlyTrax [36]. These orientation voltages, alongside the camera frame triggers and information about visual stimuli presented, were digitized at 1 kHz using a Digidata 1440a (Molecular Devices).

Data were processed using custom Python software that extracted the offset of each trial by subtracting the center of stimulus position from fly orientation. “Fixation” was calculated by measuring the percentage of time within 3-15 s of stimulus onset spent with an offset between −45° and 45°. We chose this 90° window because it equaled the amplitude of stimulus movement (60°), plus 2 stimulus widths (30° = 2*15°) to allow for potential switches of fixation from edge to edge. “Antifixation” was calculated by measuring the percentage of time within 3-15 s of stimulus onset spent with an offset greater than −135° or 135°, chosen to be opposite to the fixation window. Scores of all trials of each shape were averaged to obtain one score per shape per fly. Because not all flies experienced all four analyzed shapes, we treated fixation scores of the shapes as independent groups for statistical purposes. Heatmaps of offsets from trials, separated by shape, show orientation toward the long stripe and away from the spot. Each sector represents 15° x 1 s and are normalized by column.

Mosquito Magnetic Tethering

For experiments in Figures 1, S1, and S2, and Video S1 female mosquitoes were collected 4-15 days after eclosion and fasted in the presence of a water source comprising a 60 mL glass bottle (Fisherbrand Clear Boston Round Bottles Without Cap Fisher Sci Cat# 02-911-944) filled with deionized water and plugged with a water-soaked cotton wick (Richmond Dental Braided Rolls ½” x 6,” Catalogue # 201205) for 18-25 hr. Mosquitoes were anesthetized on ice (4°C) for 5-35 min and were attached by the dorsal part of their prothorax to a steel pin (0.20 mm Minutiens cut to 4-6 mm height, Austerlitz) using blue-light activated glue (Bondic, Canada). For 1-4 hr after tethering, mosquitoes recovered in a dark, humid chamber while their legs lightly contacted mesh.

Mosquitoes were then suspended in a vertically-aligned magnetic field in the center of a cylindrical LED display (525 nm, IORodeo) covering 360 in azimuth and 94 in elevation with each pixel subtending ~3.75°. LEDs were controlled using PControl in MATLAB [10]. We generated a textured background consisting of pixels randomly assigned to luminances of 10. or 40. cd m^{-2}, and we used the same background in the same position for all trials. The long stripe, medium stripe, spot, and blank as used in the fly trials were pseudorandomly presented in 10-15 s trials, with every 8 trials interspersed by 10-15 s of moving the background alone. The long stripe, medium stripe, spot, and blank were superimposed on the background at a random position, moving in a sinusoid of peak-to-peak amplitude 60° and frequency randomly chosen from 0, 0.1, 0.5, and 1 Hz. Mosquitoes that failed to follow the direction of wide-field motion or failed to sustain flight were discarded.

To obtain body orientation, mosquitoes were lit from below with IR LEDs (850 nm, DigiKey) were captured with an infrared-sensitive camera (Point Grey FL3-GE-03S1M-C) triggered externally, recording frames (648 × 488 pixels) at 100 Hz. Mosquito body orientation was extracted from camera images in real time using FView and FlyTrax [36]. Camera frame triggers and information regarding the visual stimuli presented were digitized at 1 kHz using a DAQ (Measurement Computing USB-204) and DAQFlex software (Measurement Computing).

Throughout all magnotether experiments, breathing air (~0.04% CO_2, Praxair AI BR-KN) was pumped into the box via a diffusion pad (59-144, http://Flystuff.com) installed on the ceiling of the enclosure, 20.5 cm directly above the position of the tethered mosquito. In trials labeled “CO_2” (Figure 1K), the air stream was switched to 10% CO_2 (Praxair AI CD10C-K) via a solenoid valve (Parker-Hannifin) for 10 s. To maintain the same CO_2 concentration throughout the experiment, 1 s of 10% CO_2 was puffed in for every 200 s of air. This regime increased the concentration of CO_2 in the mosquito tethering position 1,250 ppm above baseline and maintained it there for up to 15 min, as measured with a Carbocap Hand-Held CO_2 Meter (model GM70, Vaisala). Data recording began approximately 1-2 minutes after the initial 10 s pulse of CO_2. After each CO_2 trial, the enclosure was opened for at least 5 minutes, which as measured was sufficient to bring down CO_2 to baseline levels. In Figure 1K, because different mosquitoes experienced the air and CO_2 conditions, we treated fixation scores as independent groups for statistical purposes.

Data were processed using custom Python software that synchronized orientation data and DAQ data using computer timestamps, then processed the same way as fly magnetic tether data. Because all mosquitoes experienced all four analyzed shapes, we treated fixation scores of the shapes as dependent groups for statistical purposes. In heatmaps of offset, each sector represents 15° x 1 s and are normalized by column. Summary fixation data are shown as median with each data point representing an individual mosquito.

Glytube Blood-Meal Feeding

For experiments in Figures 1, S1, and S2, females were fed sheep blood or saline in groups of 20–50 using Glytube membrane feeders as described [39]. The protein-free saline meal contained 110 mM NaCl, 20 mM $NaHCO_3$, and 1 mM ATP. Glytubes were placed on top of mesh on the mosquito cage, and females were allowed to feed through the mesh for 15 min. Fed females were scored by eye for complete engorgement. Partially-fed females were treated as non-fed and discarded. Blood-fed and saline-fed females were returned to standard rearing conditions. For the "48 hr post-meal" condition, mosquitoes were fasted in the presence of a water source 20-26 hr before testing and then tested 44-52 hr after Glytube feeding. For the "96 hr post-meal" condition, mosquitoes were fasted without a water source 23-49 hr before testing and tested 94-103 hr after Glytube feeding. Water was not provided because this would stimulate females to lay eggs, and the experimental design required females to be gravid at the time of testing.

Heat-Seeking Assay

Experiments in Figures 2, 3, S3, and S4 were performed as previously described [4]. Briefly, the assay apparatus is a 30 × 30 × 30 cm Plexiglass box with a 6 × 9 cm Peltier element (Tellurex) on one vertical wall. To affix a visual stimulus to the Peltier, a 2 cm black dot representing 5.42% of the Peltier area was printed onto a piece of standard white letter size printer paper (extra bright, Navigator; Office Depot/Office Max), which was cut to 15 × 17 cm and held taut over the Peltier by a magnetic frame such that the center of the dot was 13.97 cm above the ground. Because mosquitoes in free flight can change their perceived angular size of the dot by changing their position, it is difficult to make exact comparisons to the static angular sizes of the stimuli presented in the magnotether. The minimum size of the dot (a mosquito as far away from the dot as possible in the assay) was 2.78°. For a mosquito to experience the dot as the same angular height as the magnotether square (15°), the dot would be 7.60 cm directly ahead of her; for the medium stripe (46°), 2.36 cm; for the long stripe (94°), 0.93 cm.

For blank control trials in Figures 2 and S3, the paper was turned over to show the unprinted side. This was done to control for the effect of the Xerox Phaser solid printer ink used to generate the dot, which we speculated might affect heat transfer at that position on the paper. Although the dot was faintly visible to the human eye, mosquitoes showed little or no preference for that position on the paper, and there were no detectable differences in the thermal image of the Peltier when the dot was in place (Figure 2C). All stimulus periods lasted 3 min, followed by 9 min of ambient temperature. CO_2 pulses (20 s) accompanied all stimulus period onsets. A second identical control Peltier element was situated on the wall opposite to the stimulus Peltier and was set to ambient temperature during all experiments. In Figure 2, air temperature was measured using a controller and thermocouple identical to that used to measure internal Peltier temperature (Oven Industries 5R7-570, Oven Industries TR91-170). The thermocouple was placed at the center of the Peltier and 2 mm from the Peltier surface, approximating the distance of a mosquito's center of mass from the surface when landed.

Female mosquitoes were separated 8-12 days after eclosion from mixed-sex cages and sorted at 4°C into groups of 45-50. They were kept in custom canisters and sugar-starved in the presence of a water source 13-24 hr before testing. Experiments in Figures 3 and 4 were double-blinded to genotype. For each trial, one group was introduced into the enclosure, and only mosquitoes directly on the Peltier area (Figure 2B) were scored. Due to low contrast between the dark mosquitoes and the black dot, each frame for each experiment in Figures 2, 3, S3, and S4 was manually inspected to ascertain the number of mosquitoes on the dot.

Summary data are shown as median with individual data points, and timeseries data are shown as median with range of median absolute deviation with normalization constant 1.4826, a robust estimator of dispersion [40, 41]. For the normalized timeseries data shown in Figure 3C, for each heat bout within each trial we computed the mean occupancy on the Peltier during the minute before heat onset and divided the rest of the timeseries by that mean, such that the data are represented as percentages of initial occupancy before heat. Heatmaps are smoothed 2D histograms of mean mosquito occupancy during seconds 90–180 of stimulus periods, sampled at 1 Hz and binned into 12 × 16 image sectors.

We quantified positions of landings and takeoffs (Figure 4) by superimposing two consecutive frames and manually looking for differences. A still mosquito would appear as a completely overlapped image, whereas a walking mosquito would appear as two adjacent images, defined here as two mosquito images that either shared the same orientation and were less than one mosquito body length apart or had orientations with a difference of less than 90° and shared a center of rotation. A mosquito that was present in the first frame but not in an adjacent image in the second frame was counted as a "takeoff." Conversely, a mosquito present in the second frame but not the first was counting as a "landing" (Figure 4A). Because we sampled at 1 Hz, it is possible that a seemingly walking or still mosquito represents a mosquito that took off in the first frame and then another mosquito that landed within 1 s in the same or an adjacent location. But we expect that such an event would be exceedingly rare. Thus, this manual quantification represents a conservative estimate of landings and takeoffs. Frames were scored blind to genotype.

Because we did not track individual mosquito identity, we could not track duration of individual dwelling events. However, given the times of landing and takeoff events, we reasoned that we could deduce a mean population dwell time as follows (Figure 4B). Let A = landing time, B = takeoff time. B – A thus represents dwell time.

$$\boldsymbol{Mean}(\boldsymbol{B}-\boldsymbol{A})=\frac{\sum_{n=1}^{k}(\boldsymbol{B}_n-\boldsymbol{A}_n)}{\boldsymbol{k}}$$

$$Mean(B - A) = \frac{\sum_{n=1}^{k}(B_n) - \sum_{n=1}^{k}(A_n)}{k}$$

To make this calculation, we assigned all mosquitoes present at the start of the heat epoch a landing time of 0 s and all mosquitoes present at the end of the heat epoch a takeoff time of 180 s.

QUANTIFICATION AND STATISTICAL ANALYSIS

All statistical analysis was performed using the Python package scipy.stats. Kruskal-Wallis test with post hoc Mann-Whitney test was used to compare more than 2 independent groups, and Friedman's test for repeated-measures with post hoc Wilcoxon matched-pairs signed-rank test was used to compare more than 2 dependent groups. Mann-Whitney U test was used to compare 2 independent groups. Post hoc tests included Bonferroni correction when multiple comparisons were made. Details of statistical methods are reported in the figure legends.

DATA AND CODE AVAILABILITY

Data file containing all raw magnotether data, all processed data, and all code used to process data in this paper are available at https://github.com/VosshallLab/LiuVosshall2019

Due to file size limitations of online data repositories, raw image files from the heat-seeking assay are available upon request.